IEEE Access
Multidisciplinary | Rapid Review | Open Access Journal

Received June 5, 2021, accepted June 30, 2021, date of publication July 5, 2021, date of current version July 13, 2021.

Digital Object Identifier 10.1109/ACCESS.2021.3094540

SCH: A Speed Measurement Method of Combined Hyperbolic Frequency Modulation Signals

PENG LIU[1] AND CAIXIA SONG[2]
[1]Hangzhou Institute of Applied Acoustics, Hangzhou 310023, China
[2]College of Science and Information, Qingdao Agricultural University, Qingdao 266109, China

Corresponding author: Caixia Song (cassiesong@qau.edu.cn)

This work was supported in part by the Shandong Smart Ocean Ranch Engineering Technology Collaborative Innovation Center, in part by the Research Fund for High-Level Talents of Qingdao Agricultural University under Grant 1119048, in part by the Shandong Agricultural Science and Technology Service Project under Grant 2019FW037-4, in part by the Shandong Technology Innovation Guidance Program under Grant 2020LYXZ023, in part by the Horizontal Project under Grant 20193702010792, in part by the Experimental Technical Project of Qingdao Agricultural University under Grant SYJK18-01, and in part by the Ministry of Education Industry-University Cooperation Collaborative Education Project under Grant 201902005027 and Grant 201901029013.

ABSTRACT Hyperbolic Frequency Modulation (HFM) signal has certain tolerance to Doppler shift. However, during ranging, the unidirectional modulated HFM signal cannot eliminate the Doppler delay at the output of the matched filtering, and thus there is a ranging error. After the combined positive and negative HFM echo signals are matched and filtered, the Doppler-induced delay is closely related and proportional to the frequency, bandwidth and pulse width of the transmitted signals. By using the combined signals, the ranging error in the ranging of single modulated HFM signal can be eliminated. In this paper, a Speed measurement method of Combined HFM signals (SCH) is proposed, which employs positive and negative frequency modulation signals for speed measurement and ranging. Moreover, the SCH method relaxes the requirements of bandwidth and pulse width, which makes it more suitable for general conditions. Extensive simulation results show that the proposed approach can better estimate the speed and distance of moving targets, and it has reference value for engineering application.

INDEX TERMS Hyperbolic frequency modulation, Doppler invariance, speed measurement.

I. INTRODUCTION

Sonar plays a pivotal role in ocean exploration. As countries continue to increase their investment in submarine noise reduction technology, which has led to the rapid development of noise reduction technology. The radiated sound source level of submarine is decreasing at the speed of 1dB every year [1]. As a result, the passive detection capability is severely limited, and the passive detection is becoming more and more difficult. Therefore, active detection is becoming a new development trend.

Linear Frequency Modulation (LFM) is a commonly used signal in radar detection. The fuzzy function of LFM signal is an Oblique blade type [2], [3]. Since the radar uses a high-frequency signal, the Doppler shift of the target can be ignored relative to the frequency of the signal itself. However, the detection frequency of sonar in the water is low. When the Doppler shift produced by the moving target is too large, the spectrum of the LFM echo signal will be mismatched with the matched filter, which will lead to the loss of the matching gain and thus the detection performance decreases.

The waveform of Hyperbolic Frequency Modulation (HFM) signal is insensitive to Doppler, which can make up for the shortcomings of LFM signal. And thus, HFM signals are widely used in the fields of radar and sonar ranging and speed measurement. In [4], the influence of Doppler of moving target on HFM is introduced in detail, and a tolerant matched filter is proposed. However, how to use Doppler to measure the target speed and how to eliminate the influence of target Doppler on ranging are not analyzed in depth.

At present, the common speed measurement method for sonar is to use a single frequency signal to measure velocity. Due to the time-varying characteristics of the underwater acoustic channel, the single frequency signal for speed measurement is unstable. At certain moments, the single frequency signal will be filtered out by the underwater acoustic channel, resulting in no echo return, and the speed measurement thus cannot be achieved. There is also sonar that uses

The associate editor coordinating the review of this manuscript and approving it for publication was Chengpeng Hao.

multiple sets of Doppler matched filters to match [3]. With the improvement of speed measurement accuracy, the cost increases exponentially.

In order to overcome the above limitations of speed measurement and ranging, a Speed measurement method of Combined Hyperbolic frequency modulation signals (SCH) is proposed, which employs positive and negative frequency modulation signals (HFM+HFM) for speed measurement and ranging. SCH method can not only measure speed accurately, but also solve the range error caused by Doppler shift in unidirectional modulation HFM. The main contributions of this paper are fourfold:

1) The SCH method makes full use of the Doppler characteristic of the moving target and the time delay relationship of the combined signals. Based on the time-delay relationship, the accurate velocity of the target can be obtained.

2) The SCH method can achieve accurate speed measurement without adding filter banks and additional hardware equipment, and the measurement cost is thus greatly reduced.

3) The SCH method employs the combined HFM signals to measure velocity, and the combined HFM signals have a certain frequency bandwidth. Even if some frequency points are filtered out by the underwater acoustic channel, there still be some echoes arriving, and the speed can still be measured. The SCH method overcomes the shortcomings of single frequency signal for speed measurement and has better adaptability to ocean channels.

4) In the combined HFM signals proposed in this paper, the two HFM signals can be freely combined, and the frequency band and pulse width can be independently configured, which makes full use of the frequency band and pulse width resources. Moreover, the SCH method is simple to implement, and has engineering application value.

In our previous work [5], we propose a Joint Linear frequency modulation and Hyperbolic frequency modulation approach for Speed measurement (JLHS), which employs the same frequency band of positive and negative frequency modulation signals (LFM+HFM) for speed measurement and ranging. Compared with JLHS, in the SCH method, the two HFM signals do not need to be completely consistent, which relaxes the requirements of bandwidth and pulse width and makes it more suitable for general conditions. On the other hand, since the tolerance of LFM to moving targets is far less than that of HFM, when the target speed is too high, LFM will have no peak output after matched filtering, and thus JLHS cannot realize ranging and speed measurement.

II. RELATED WORKS

The HFM waveform has an inherent Doppler-invariant property. In order to apply the HFM waveform to existing inverse synthetic aperture radar imaging systems, Wei *et al.* [6] proposed a new pulse compression algorithm. the pulse compression is accomplished by space-variant phase compensation. In addition, the space-variant phase compensation is realized by resampling and fast Fourier transform with high computational efficiency. Doisy *et al.* [7] derived the expressions of Doppler tolerance, Doppler and delay accuracy, and delay-Doppler ambiguity in case of high bandwidth duration product signals. The replicas of Doppler estimation and target range were reduced. Finally, results were applied to low-frequency active sonar. Wang *et al.* [8] presented a method by employing the HFM signal as a channel probe to make Doppler estimation and timing synchronization simultaneously. Yang *et al.* [9] demonstrated that the acceleration of the target results in a frequency shift which is the source of the signal distortion under the assumption that the acceleration is constant and along the direction of the velocity. Therefore the frequency-shifted version of the matched filter can be applied to eliminate the mismatch between the reflected signal and the matched filter caused by the acceleration of the target. Lee *et al.* [10] proposed an underwater acoustic communication with hyperbolic frequency modulated waveforms. The received signal was demodulated by matched filtering of received signal and one hyperbolic chirp pulse. Simulation was performed to evaluate the performance of the proposed method. Wei *et al.* [11] developed a fast method for generating HFM radar echoes using static electromagnetic data for HFM waveforms in wideband radar imaging with the computational complexity effectively reduced by phase-matched filtering and frequency domain down-sampling. The result was used to study the influence to HFM signal matched filtering for high-speed movements. This method was also suitable for LFM waveforms. Simulations verified the accuracy and effectiveness of this method. Besson *et al.* [12] dealt with parameter estimation of product signals consisting of HFM and chirp factors, and presented a computationally simple algorithm that decouples estimation of the chirp parameters from those of the HFM part. Wang *et al.* [13] proposed a method to estimate the target velocity using a combination of two HFM signals. They found that a HFM with an increasing frequency sweep (positive HFM) and one with a decreasing frequency sweep (negative HFM) yield a different time. And a better Doppler estimation can be obtained by using a negative HFM signal followed by a positive HFM signal than the other way around. The method was applied to real data and performance was demonstrated via simulated data. Murray [4] introduced an extended matched filter for HFM waveforms in active sonar systems, along with an exact closed-form solution for the Doppler bias in time of arrival estimates when using this filter. This solution applied to both broadband and narrowband HFM signals. Recently, the hyperbolic-frequency modulated signal has been widely employed in sonar systems for moving targets due to its Doppler tolerance, while the precise velocity estimation becomes a great challenge under such conditions. Kim *et al.* [14] investigated the performance of HFM signals for timing synchronization in underwater acoustic communication systems. The synchronization performance of the proposed HFM was then evaluated numerically using the channel model constructed based on western sea of South Korea. Numerical analysis suggests the HFM design achieving good performance for timing synchronization in presence

of Doppler scale. Diamant *et al.* [15] presented a method for Doppler-shift estimation based on comparing the arrival times of two chirp signals and approximating the relation between this time difference and the Doppler shift ratio. This analysis also provides an interesting insight about the resilience of chirp signals to Doppler shift. The simulation results demonstrate improvement compared to commonly used benchmark methods in terms of accuracy of the Doppler shift estimation at near-Nyquist baseband sampling rates. Lee *et al.* [16] proposed a new fast target detection method that was robust to the variation of unknown target speed. The proposed method secured a Signal-to-Noise Ratio (SNR), approaching that of the optimal matched filter output, that was also robust to the variation of target speed and thus it was very useful for the practical use in antitorpedo torpedoes or supercavitating underwater missiles that need to equip low-complexity and robust signal processing systems. Huang *et al.* [17] proposed an effective iterative method for parameter estimation of multipath echo. The proposed method retrieves a signal component by searching for the optimal scale factor from the resampling matching outputs, and eliminates the matching output of the estimated signal to analyze the next component. The method prevented the time-domain subtractions of the received signals for providing a higher robustness. Therefore, it can be applied in many fields including active target detection and underwater communication.

III. HYPERBOLIC FREQUENCY MODULATION (HFM) SIGNAL WAVEFORM

Let T, f_0, f_1 and $s_s(t)$ represent the pulse width of the HFM signal, the starting frequency of the HFM signal, the ending frequency of the HFM signal and the HFM transmitting signal changing over time, respectively. Then, $s_s(t)$ can be expressed as follows:

$$s_s(t) = \begin{cases} e^{j\frac{2\pi}{b}\ln(1+bf_0t)} & 0 \le t \le T \\ 0 & otherwise \end{cases} \tag{1}$$

where b denotes frequency modulation coefficient and $b = \frac{f_0 - f_1}{f_0 f_1 T}$.

When $f_1 > f_0$, the HFM signal is called positive hyperbolic frequency modulation, denoted as HFM^+. When $f_0 > f_1$, the HFM signal is called negative hyperbolic frequency modulation, denoted as HFM^-.

IV. DOPPLER INVARIANCE PRINCIPLE OF HFM

Instantaneous frequency is used to describe the changing nature of unstable waveforms. Let $\phi(t)$ denote instantaneous phase of HFM transmitting signal and $\phi(t) = \frac{1}{b}\ln(1 + bf_0t)$ Based on Equation (1), the instantaneous frequency $f_s(t)$ of HFM transmitting signal can be calculated as

$$\begin{aligned} f_s(t) &= \frac{d\phi(t)}{dt} \\ &= \frac{d(\frac{1}{b}\ln(1+bf_0t))}{dt} \\ &= \frac{f_0}{1+bf_0t} \end{aligned} \tag{2}$$

Let v denote the speed of the target. When the target moves at speed v, the relative motion between the sonar and the target causes the transmitted signal with the pulse width T. And at the receiving point, the transmitted signal becomes a signal with a pulse width $\frac{T}{\eta}$. Therefore, the pulse width of the echo is linearly compressed or stretched η times. η can be calculated by

$$\eta = \frac{c+v}{c-v} \tag{3}$$

where c represents the speed of sound in water and $c = 1500$m/s.

Let $s_r(t)$ represent the received echo signal. Due to the radial movement between the target and the sonar platform, $s_r(t)$ can be calculated as

$$s_r(t) = \begin{cases} e^{j\frac{2\pi}{b}\ln(1+bf_0\eta t)} & 0 \le t \le T \\ 0 & otherwise \end{cases} \tag{4}$$

Let $\varphi(t)$ and $f_r(t)$ represent the instantaneous phase of the received echo signal and the instantaneous frequency of the received echo signal, respectively. We have

$$\begin{aligned} f_r(t) &= \frac{d\varphi(t)}{dt} \\ &= \frac{d(\frac{1}{b}\ln(1+bf_0\eta t))}{dt} \\ &= \frac{f_0\eta}{1+bf_0\eta t} \end{aligned} \tag{5}$$

Since the HFM signal is insensitive to Doppler, the HFM signal has the characteristic of Doppler invariance [18]. Moreover, the change rule of the instantaneous frequency of the received signal remains unchanged, except that the instantaneous frequency $f_s(t)$ of the original signal is shifted by a time t_0, where t_0 represents matched filter delay caused by target Doppler. We have

$$f_s(t - t_0) = f_r(t) \tag{6}$$

Substitute $f_s(t)$ and $f_r(t)$ into Equation (6), we have

$$\frac{f_0}{1+bf_0(t-t_0)} = \frac{f_0\eta}{1+bf_0\eta t} \tag{7}$$

Based on Equation (7), t_0 can be computed as

$$t_0 = \frac{f_1(\frac{1}{\eta} - 1)T}{f_1 - f_0} \tag{8}$$

There are two main factors to consider when HFM signals are used for target detection: frequency band and pulse width. We employ two HFM signals to obtain the delay difference and the delay ratio after matched filtering.

HFM signal 1 (HFM1): The starting frequency, ending frequency and pulse width are f_{10}, f_{11} and T_1, respectively.

HFM signal 2 (HFM2): The starting frequency, ending frequency and pulse width are f_{20}, f_{21} and T_2, respectively.

HFM1 and HFM2 can be freely combined, and the frequency band and pulse width can be independently configured. That is, there is no size limit between HFM1 and HFM2. Moreover, there is no size limit between f_{l0} and f_{l1}, that is, both $f_{l0} >= f_{l1}$ and $f_{l1} >= f_{l0}$ are allowed. On the other hand, there is also no size limit between f_{20} and f_{21}, that is, both $f_{20} >= f_{21}$ and $f_{21} >= f_{20}$ are allowed.

Moving target for FM signal, time delay t_{delay_1} of HFM1 and time delay t_{delay_2} of HFM2 can be calculated as Equation (9) and Equation (10), respectively.

$$t_{delay\_1} = \frac{f_{11}(\frac{1}{\eta} - 1)T_1}{f_{11} - f_{10}} \tag{9}$$

$$t_{delay\_2} = \frac{f_{21}(\frac{1}{\eta} - 1)T_2}{f_{21} - f_{20}} \tag{10}$$

Let t_d denote the difference between t_{delay_1} and t_{delay_2}, we have

$$\begin{aligned} t_d &= t_{delay\_1} - t_{delay\_2} \\ &= \frac{f_{11}(\frac{1}{\eta} - 1)T_1}{f_{11} - f_{10}} - \frac{f_{21}(\frac{1}{\eta} - 1)T_2}{f_{21} - f_{20}} \end{aligned} \tag{11}$$

Let t_r denote the ratio of t_{delay_1} and t_{delay_2}, we have

$$t_r = \frac{t_{delay\_1}}{t_{delay\_2}} = \frac{\frac{f_{11}T_1}{f_{11} - f_{10}}}{\frac{f_{21}T_2}{f_{21} - f_{20}}} \tag{12}$$

V. THE REALIZATION OF SPEED MEASUREMENT AND RANGING

Now let's derive the speed measurement formula. We assume that the movement speed v of the target is positive toward the sonar system. Two combined HFM signals: HFM1 and HFM2 are transmitted. Let t_1 and t_2 represent the time of maximum matched filter of HFM1 and the time of maximum matched filter of HFM2, respectively. We have

$$\begin{cases} t_1 = \dfrac{2R}{c} + t_{delay\_1} \\ t_2 = \dfrac{2R}{c} + t_{delay\_2} \end{cases} \tag{13}$$

According to Equation (13), we have

$$\begin{aligned} t_1 - t_2 &= \frac{f_{11}(\frac{1}{\eta} - 1)T_1}{f_{11} - f_{10}} - \frac{f_{21}(\frac{1}{\eta} - 1)T_2}{f_{21} - f_{20}} \\ &= t_{delay\_1} - t_{delay\_2} \end{aligned} \tag{14}$$

Based on Equation (3) and Equation (14), we have

$$v = -\frac{\frac{t_1 - t_2}{\frac{f_{11}T_1}{f_{11} - f_{10}} - \frac{f_{21}T_2}{f_{21} - f_{20}}}}{\frac{t_1 - t_2}{\frac{f_{11}T_1}{f_{11} - f_{10}} - \frac{f_{21}T_2}{f_{21} - f_{20}}} + 2} \times c \tag{15}$$

To simplify the formula, let

$$x = \frac{t_1 - t_2}{\frac{f_{11}T_1}{f_{11} - f_{10}} - \frac{f_{21}T_2}{f_{21} - f_{20}}} \tag{16}$$

Therefore, we have

$$v = -\frac{xc}{x + 2} \tag{17}$$

According to Equation (12) and Equation (13), we have

$$R = \frac{c}{2} \times \frac{t_1 - \frac{\frac{f_{11}T_1}{f_{11} - f_{10}}}{\frac{f_{21}T_2}{f_{21} - f_{20}}} \times t_2}{1 - \frac{\frac{f_{11}T_1}{f_{11} - f_{10}}}{\frac{f_{21}T_2}{f_{21} - f_{20}}}} \tag{18}$$

To simplify the formula, let

$$y = \frac{\frac{f_{11}T_1}{f_{11} - f_{10}}}{\frac{f_{21}T_2}{f_{21} - f_{20}}} \tag{19}$$

Therefore, we have

$$R = \frac{t_1 - yt_2}{1 - y} \tag{20}$$

In the HFM pulse train, the time of maximum value of the matched filter output of the signal in the first frequency band, such as HFM1, is time t_1. And the time of maximum value of the matched filter output of the signal in the second frequency band, such as HFM2, is time t_2. The movement direction of the target is determined by the calculated positive value and negative value. We can derive the conclusions as follows:

1) When the pulse width in the pulse train group is the same ($T_1 = T_2$), Equation (15) and Equation (18) can be rewritten as Equation (21) and Equation (22), respectively.

$$v = -\frac{\frac{t_1 - t_2}{\frac{f_{11}}{f_{11} - f_{10}} - \frac{f_{21}}{f_{21} - f_{20}}}}{\frac{t_1 - t_2}{\frac{f_{11}}{f_{11} - f_{10}} - \frac{f_{21}}{f_{21} - f_{20}}} + 2T_1} \times c \tag{21}$$

$$R = \frac{c}{2} \times \frac{t_1 - \frac{\frac{f_{11}}{f_{11} - f_{10}}}{\frac{f_{21}}{f_{21} - f_{20}}} \times t_2}{1 - \frac{\frac{f_{11}}{f_{11} - f_{10}}}{\frac{f_{21}}{f_{21} - f_{20}}}} \tag{22}$$

2) When the frequency band in the pulse train group is the same ($f_{10} = f_{20}, f_{11} = f_{21}$), Equation (15) and Equation (18) can be rewritten as Equation (23) and Equation (24), respectively.

$$v = -\frac{\frac{t_1 - t_2}{T_1 - T_2}}{\frac{t_1 - t_2}{T_1 - T_2} + \frac{2f_{11}}{f_{11} - f_{10}}} \times c \tag{23}$$

$$R = \frac{c}{2} \times \frac{t_1 - \frac{T_1}{T_2} \times t_2}{1 - \frac{T_1}{T_2}} \tag{24}$$

Now we compute the time complexity of the proposed SCH method. In SCH method, after each single HFM signal (HFM+HFM) is transmitted separately, the received echo signals and the transmitted signals are matched and filtered to obtain the target velocity and range information of the target. When the combined HFM signals are transmitted separately, the space complexity is $O(1)$ and the time complexity is also $O(1)$. When the echo signals are matched and filtered, the copy signals are combined signals, and both the space complexity and the time complexity are $O(1)$.

VI. PERFORMANCE ANALYSIS

The ideal transmission channel is an infinite space composed of lossless and uniform medium, and the signal will not have any distortion during the propagation process. However, the sea water medium space is a lossy heterogeneous medium space. In addition to general absorption and diffusion, the signal in sea water is also affected by multi-path effect, channel time-varying and fluctuation effect, which result in the broadening of the echo and the difficulty in distinguishing the echo position of the combined echo signal. In order to achieve accurate speed measurement, the time difference t_d between t_1 and t_2 should be as large as possible.

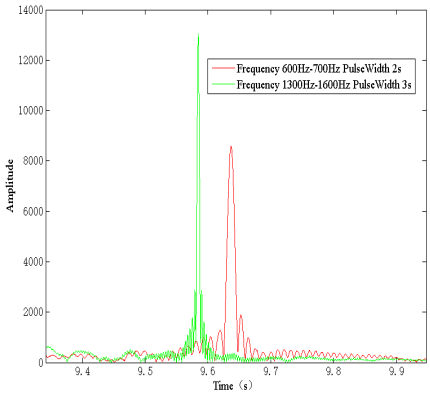

(a) v = -20m/s

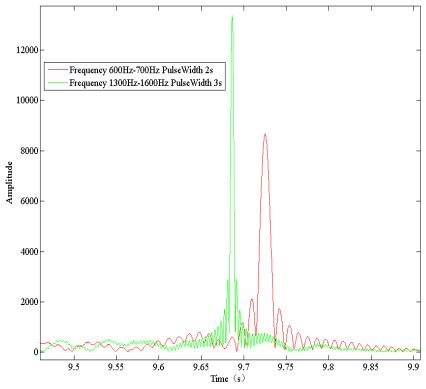

(b) v = -15m/s

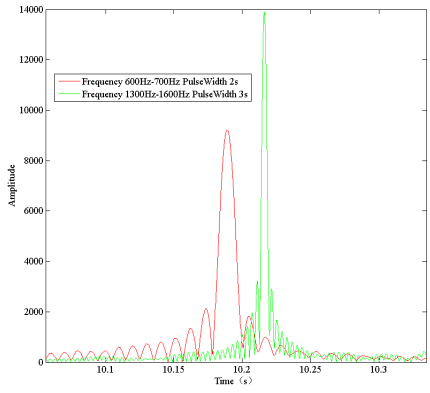

(c) v = 10m/s

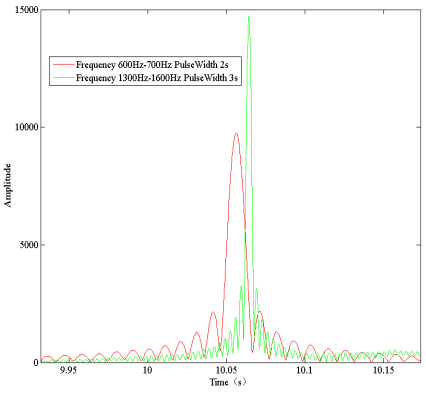

(d) v = 3m/s

FIGURE 1. **The output of matched filtering at various *v* under Simulation Environment 1.**

We rewrite the Equation (11) as follows:

$$\begin{aligned} t_d &= t_{delay\_1} - t_{delay\_2} \\ &= \frac{f_{11}(\frac{1}{\eta}-1)T_1}{f_{11}-f_{10}} - \frac{f_{21}(\frac{1}{\eta}-1)T_2}{f_{21}-f_{20}} \\ &= (\frac{1}{\eta}-1)\times\left(\frac{f_{11}T_1}{f_{11}-f_{10}} - \frac{f_{21}T_2}{f_{21}-f_{20}}\right) \end{aligned} \tag{25}$$

Let bandwidth $B_1 = f_{11} - f_{10}$ and bandwidth $B_2 = f_{21} - f_{20}$. Let K denote modulation rate of change, and $K = \frac{B}{T}$. Then $K_1 = \frac{B_1}{T_1}$ and $K_2 = \frac{B_2}{T_2}$. Therefore, $t_{delay\_1} - t_{delay\_2} = (\frac{1}{\eta} - 1)\frac{f_{11}}{K_1} - \frac{f_{21}}{K_2}$. Since $\eta = \frac{c+v}{c-v}$ is a constant, then $(\frac{1}{\eta} - 1)$ is also a constant. $f_{11} > 0$ and $f_{11} > 0$. We have

$$t_{delay\_1} - t_{delay\_2} = (\frac{1}{\eta} - 1) \times (\frac{f_{11}}{K_1} - \frac{f_{21}}{K_2}) \tag{26}$$

After the transmitted signals are determined, Equation (14) can be used to judge whether the configuration of the combined signals is reasonable. Once configuration is not suitable, the modulation rate K and frequency f of the combined signal can be adjusted timely.

Since the sign of the modulation change rate K of the positive and negative FM is opposite, the $t_{delay\_1} - t_{delay\_2}$ difference is bigger, which is more conducive to detection. During sonar detection, when the target movement speed is constant, the higher the detection frequency, the greater the Doppler shift caused. Therefore, the delay is more obvious. So high-frequency sonar is easier to measure speed than low-frequency sonar is.

VII. SIMULATION AND VERIFICATION

A. SIMULATION SETTINGS

We set up three simulation environments for performance analysis: Simulation Environment 1, Simulation Environment 2 and Simulation Environment 3.

Simulation Environment 1: In the HFM signal 1, the starting frequency, the ending frequency and pulse width are $f_{10} =$ 600Hz, $f_{11} =$ 700Hz and $T_1 =$ 2s, respectively. In the HFM signal 2, the starting frequency, the ending frequency and pulse width are $f_{20} =$ 1300Hz, $f_{21} =$ 1600Hz and $T_2 =$ 3s, respectively. For both two HFM signals, the sample frequency $f_{sa} =$ 7000Hz, SNR is $-$20dB, and the distance between the target and the sound source is 7.5km.

Simulation Environment 2: In the HFM signal 1, the starting frequency, the ending frequency and pulse width are $f_{10} =$ 2000Hz, $f_{11} =$ 1000Hz and $T_1 =$ 3s, respectively. In the HFM

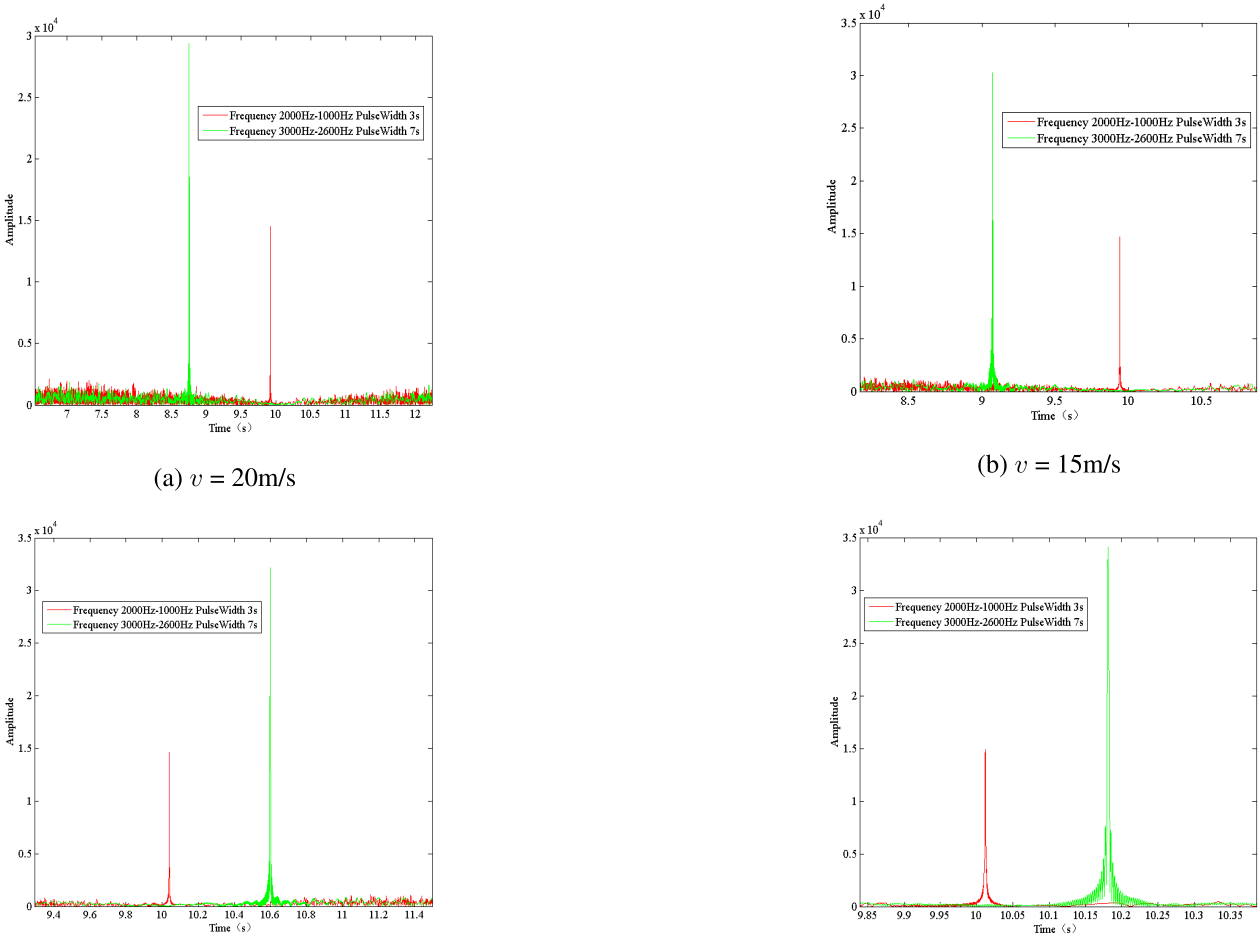

(a) v = 20m/s

(b) v = 15m/s

(c) v = -10m/s

(d) v = -3m/s

FIGURE 2. The output of matched filtering at various v under Simulation Environment 2.

TABLE 1. Comparison of simulation results under Simulation Environment 1.

Speed v (m/s)	Echo time of combined signals (s)		Ranging (km)	Speed measurement (m/s)	Speed measurement error of SCH	Ranging error of SCH	Ranging error of single signal		Range accuracy improvement ratio	
	HFM signal 1	HFM signal 2					HFM signal 1	HFM signal 2	Compared to HFM signal 1	Compared to HFM signal 2
-20m/s	9.6362	9.5844	7.4991	-19.6799	1.6%	0.012%	3.638%	4.156%	99.670%	99.711%
-15m/s	9.7256	9.6864	7.5	-14.8455	1.03%	0%	2.744%	3.136%	100%	100%
10m/s	10.1892	10.2162	7.50015	10.0571	0.5710%	0.002%	1.892%	2.162%	99.894%	99.907%
3m/s	10.0562	10.0642	7.50015	2.994	0.2000%	0.002%	0.562%	0.642%	99.644%	99.688%

TABLE 2. Comparison of simulation results under Simulation Environment 2.

Speed v (m/s)	Echo time of combined signals (s)		Ranging (km)	Speed measurement (m/s)	Speed measurement error of SCH	Ranging error of SCH	Ranging error of single signal		Range accuracy improvement ratio	
	HFM signal 1	HFM signal 2					HFM signal 1	HFM signal 2	Compared to HFM signal 1	Compared to HFM signal 2
20m/s	9.9178	8.7534	7.49996	20.2706	1.3530%	0.00053%	0.822%	12.466%	99.935%	99.996%
15m/s	9.9388	9.0714	7.49999	15.1524	1.0160%	0.00013%	0.612%	9.286%	99.978%	99.999%
-10m/s	10.0394	10.5986	7.49996	-9.9336	0.6640%	0.00053%	0.394%	5.986%	99.865%	99.991%
-3m/s	10.012	10.1812	7.5000	-2.9918	0.2733%	0%	0.12%	1.812%	100%	100%

signal 2, the starting frequency, the ending frequency and pulse width are $f_{20} = 3000$Hz, $f_{21} = 2600$Hz and $T_2 = 7$s, respectively. For both two HFM signals, the sample frequency $f_{sa} = 7000$Hz, SNR is -20dB, and the distance between the target and the sound source is 7.5km.

Simulation Environment 3: In the HFM signal 1, the starting frequency, the ending frequency and pulse width are $f_{10} = 600$Hz, $f_{11} = 700$Hz and $T_1 = 2$s, respectively. In the HFM signal 2, the starting frequency, the ending frequency and pulse width are $f_{20} = 1900$Hz, $f_{21} = 1300$Hz and $T_2 = 3$s, respectively. For both two HFM signals, the sample frequency $f_{sa} = 7000$Hz, SNR is -20dB, and the distance between the target and the sound source is 7.5km.

B. SIMULATION RESULTS

Figure 1 shows the performance analysis under the Simulation Environment 1 under various v. Table 1 gives the numerical results of SCH. We take Figure 1(a) as an example to analyze the performance of SCH method under various speed v. From Figure 1(a), it can be seen that, after matched filtering, the combined signal echo time of HFM signal 1 and HFM signal 2 are 9.6362s and 9.5844s, respectively.

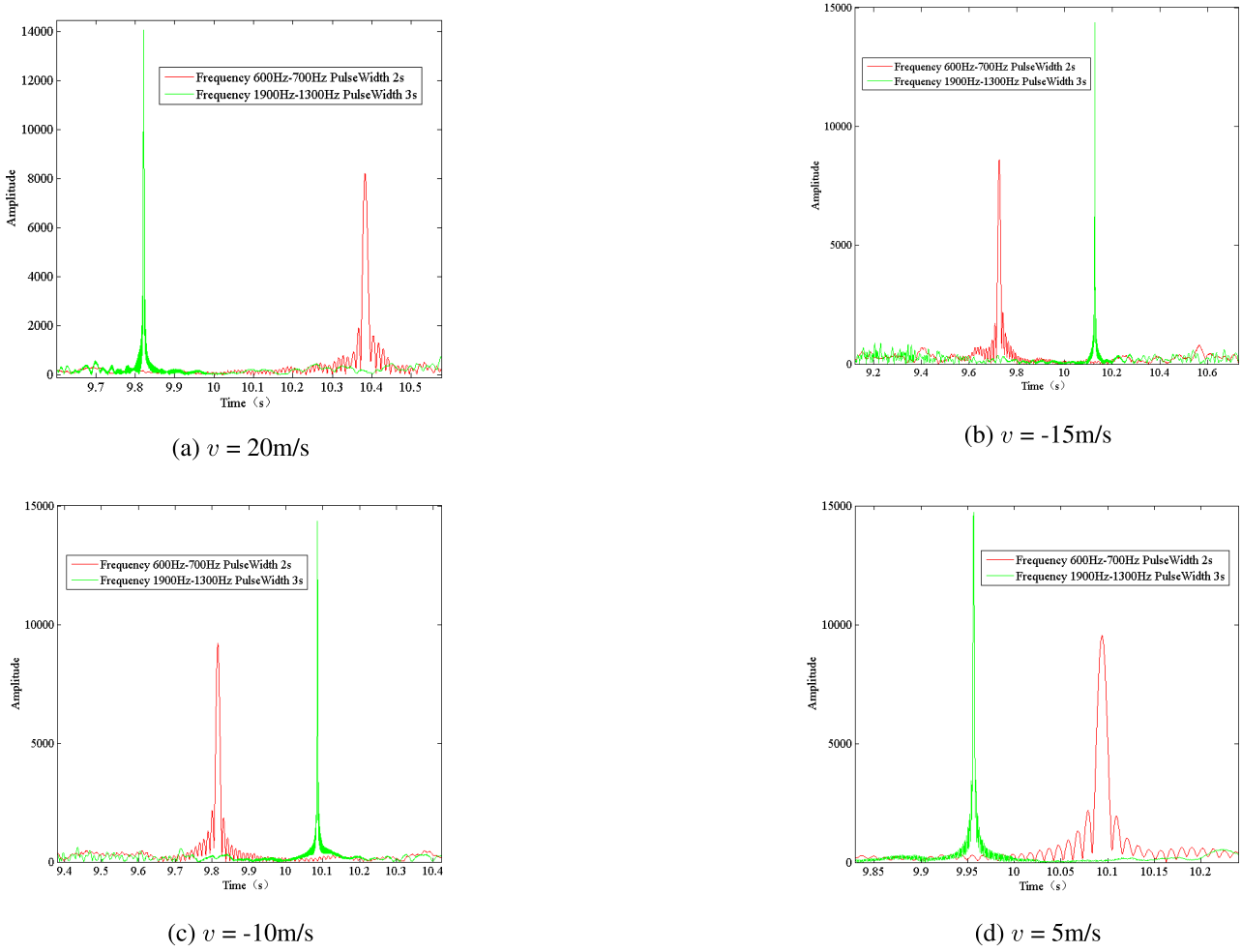

(a) v = 20m/s

(b) v = -15m/s

(c) v = -10m/s

(d) v = 5m/s

FIGURE 3. **The output of matched filtering at various v under Simulation Environment 3.**

According to Equation (15), the value of v is -19.6799m/s. It can be seen from Table 1 that, the speed measurement error and the ranging error of SCH are 1.6% and 0.012%, respectively. The ranging error of single HFM signal 1 and single HFM signal 2 are 3.638% and 4.156%, respectively. Compared with single HFM signal 1 and single HFM signal 2, the ranging measurement accuracy of SCH is improved by 99.670% and 99.711%, respectively.

Figure 2 shows the performance analysis under the Simulation Environment 2 under various speed v. Table 2 gives the numerical results of SCH. We take Figure 2(a) as an example to analyze the performance of SCH method under various speed v. From Figure 2(a), it can be seen that, after matched filtering, the combined signal echo time of HFM signal 1 and HFM signal 2 are 9.9178s and 8.7534s, respectively. According to Equation (15), the value of v is 20.2706m/s. It can be seen from Table 2 that, the speed measurement error and the ranging error of SCH are 1.353% and 0.00053%, respectively. The ranging error of single HFM signal 1 and single HFM signal 2 are 0.822% and 12.466%, respectively. Compared with single HFM signal 1 and single HFM signal 2, the ranging measurement accuracy of SCH is improved by 99.935% and 99.996%, respectively.

Figure 3 shows the performance analysis under the Simulation Environment 3 under various speed v. Table 3 gives the numerical results of SCH. We take Figure 3(a) as an example to analyze the performance of SCH method under various speed v. From Figure 3(a), it can be seen that, after matched filtering, the combined signal echo time of HFM signal 1 and HFM signal 2 are 10.3836s and 9.822s, respectively. According to Equation (15), the value of v is 20.2687m/s. It can be seen from Table 3 that, the speed measurement error and the ranging error of SCH are 1.3435% and 0.00133%, respectively. The ranging error of single HFM signal 1 and single HFM signal 2 are 3.836% and 1.78%, respectively. Compared with single HFM signal 1 and single HFM signal 2, the ranging measurement accuracy of SCH is improved by 99.965% and 99.925%, respectively.

Based on the above analysis, it is clear that the combined HFM signals for speed measurement (SCH) method proposed in this paper can accurately calculate the target speed. When the combined signal frequency and pulse width are

TABLE 3. Comparison of simulation results under Simulation Environment 3.

Speed v (m/s)	Echo time of combined signals (s)		Ranging (km)	Speed measurement (m/s)	Speed measurement error of SCH	Ranging error of SCH	Ranging error of single signal		Range accuracy improvement ratio	
	HFM signal 1	HFM signal 2					HFM signal 1	HFM signal 2	Compared to HFM signal 1	Compared to HFM signal 2
20m/s	10.3836	9.822	7.5001	20.2687	1.3435%	0.00133%	3.836%	1.78%	99.965%	99.925%
-15m/s	9.7254	10.1274	7.5	-14.8529	0.9807%	0%	2.746%	1.274%	100%	100%
-10m/s	9.8158	10.0856	7.5	-9.9361	0.6390%	0%	1.842%	0.856%	100%	100%
5m/s	10.094	9.9564	7.5	5.0173	0.3460%	0%	0.94%	0.436%	100%	100%

determined, the smaller the speed of the moving target is, the more accurate the speed measurement is. On the other hand, when the target movement speed is determined, the higher the frequency of the combined signal is, the more accurate speed measurement is.

VIII. CONCLUSION AND FUTURE WORKS

In this paper, the tolerance of the HFM signal to the Doppler shift is analyzed. The unidirectional modulated HFM signal cannot eliminate the Doppler delay t_0 at the output of the matched filter during ranging, and there is a ranging error. After the combined HFM signals are matched and filtered, the Doppler-induced delay is closely related and proportional to the frequency, bandwidth and pulse width of the transmitted signals. Based on the principle that, a Speed measurement method of Combined Hyperbolic frequency modulation signals (SCH) is proposed. Extensive simulation results show that the proposed SCH method can better estimate the distance and speed of moving targets, and it relaxes the requirements of bandwidth and pulse width, which makes it more suitable for general conditions and have reference value for engineering application.

The basis of SCH method for speed measurement and ranging is that combined HFM signals can be detected after the echo signals are processed, and the peak value after matched filtering is higher than background noise. In the future, we will study the ranging and speed measurement method under too low SNR or clutter environments.

REFERENCES

[1] P. Yuhong, Y. Qi, and W. Shichuang, "Research on hyperbolic frequency modulation signal speed and ranging method," *Acoust. Elect. Eng.*, vol. 29, no. 4, pp. 21–24, 2014.

[2] C. Liu, S. Liu, C. Zhang, Y. Huang, and H. Wang, "Multipath propagation analysis and ghost target removal for FMCW automotive radars," in *Proc. IET Int. Radar Conf. (IET IRC)*, 2021, pp. 1–5.

[3] C. Pang, S. Liu, and Y. Han, "High-speed target detection algorithm based on sparse Fourier transform," *IEEE Access*, vol. 6, pp. 37828–37836, 2018.

[4] J. J. Murray, "On the Doppler bias of hyperbolic frequency modulation matched filter time of arrival estimates," *IEEE J. Ocean. Eng.*, vol. 44, no. 2, pp. 446–450, Apr. 2019.

[5] Y. Peng, C. Song, L. Qi, P. Liu, Y. Dong, Y. Yang, B. Zhang, and Z. Qi, "JLHS: A joint linear frequency modulation and hyperbolic frequency modulation approach for speed measurement," *IEEE Access*, vol. 8, pp. 205316–205326, 2020.

[6] Z. Wei, Y. Chunmao, J. Kan, L. Yaobin, and Y. Jian, "Radar echo generation for hyperbolic frequency-modulation waveforms," *J. Tsinghua Univ. (Sci. Technol.)*, vol. 55, no. 8, pp. 878–883, 2015.

[7] Y. Doisy, L. Deruaz, S. P. Beerens, and R. Been, "Target Doppler estimation using wideband frequency modulated signals," *IEEE Trans. Signal Process.*, vol. 48, no. 5, pp. 1213–1224, May 2000.

[8] K. Wang, S. Chen, C. Liu, Y. Liu, and Y. Xu, "Doppler estimation and timing synchronization of underwater acoustic communication based on hyperbolic frequency modulation signal," in *Proc. IEEE 12th Int. Conf. Netw., Sens. Control*, Apr. 2015, pp. 75–80.

[9] J. Yang and T. K. Sarkar, "Acceleration-invariant pulse compression using hyperbolic frequency modulated waveforms," in *Proc. Int. Waveform Diversity Design Conf.*, Jan. 2006, pp. 1–5.

[10] C.-E. Lee, H.-W. Lee, K.-M. Kim, W.-S. Kim, S.-Y. Chun, and S.-K. Lee, "Underwater communication with amplitude-hyperbolic frequency modulation," in *Proc. 6th Int. Conf. Ubiquitous Future Netw. (ICUFN)*, Jul. 2014, pp. 560–561.

[11] W. Zhou, C.-M. Yeh, K. Jin, J. Yang, and Y.-B. Lu, "ISAR imaging based on the wideband hyperbolic frequency-modulationwaveform," *Sensors*, vol. 15, no. 9, pp. 23188–23204, Sep. 2015.

[12] O. Besson, G. B. Giannakis, and F. Gini, "Improved estimation of hyperbolic frequency modulated chirp signals," *IEEE Trans. Signal Process.*, vol. 47, no. 5, pp. 1384–1388, May 1999.

[13] F. Wang, S. Du, W. Sun, Q. Huang, and J. Su, "A method of velocity estimation using composite hyperbolic frequency-modulated signals in active sonar," *J. Acoust. Soc. Amer.*, vol. 141, no. 5, pp. 3117–3122, May 2017.

[14] M.-S. Kim, T.-H. Im, Y.-H. Cho, K.-W. Kim, and H.-L. Ko, "HFM design for timing synchronization in underwater communications systems," in *Proc. OCEANS (Aberdeen)*, Jun. 2017, pp. 1–4.

[15] R. Diamant, A. Feuer, and L. Lampe, "Choosing the right signal: Doppler shift estimation for underwater acoustic signals," in *Proc. 7th ACM Int. Conf. Underwater Netw. Syst. (WUWNet)*, New York, NY, USA, 2012, p. 27, doi: 10.1145/2398936.2398971.

[16] D.-H. Lee, J.-W. Shin, D.-W. Do, S.-M. Choi, and H.-N. Kim, "Robust LFM target detection in wideband sonar systems," *IEEE Trans. Aerosp. Electron. Syst.*, vol. 53, no. 5, pp. 2399–2412, Oct. 2017.

[17] S. Huang, S. Fang, and N. Han, "Iterative matching-based parameter estimation for time-scale underwater acoustic multipath echo," *Appl. Acoust.*, vol. 159, Feb. 2020, Art. no. 107094.

[18] T. Tan, *Sonar Technology*. Harbin, China: Harbin Eng. Univ. Press, 2010.

PENG LIU was born in Qingdao, China, in 1980. He received the M.S. degree, in 2007.

His research interests include sonar overall design technology and underwater acoustic signal processing.

CAIXIA SONG received the B.S. degree in computer science and technology from Shijiazhuang Army Command College, Shijiazhuang, China, in 2000, the M.S. degree in computer science and technology from Shandong University, Jinan, China, in 2004, and the Ph.D. degree in computer science and technology from the Dalian University of Technology, Dalian, China, in 2018.

Her research interests include signal processing, application of artificial intelligence, big data and blockchain technology in smart agriculture, and vehicular *ad hoc* wireless network communication.